Nonlinear Magnon Polaritons

Oscar Lee,[1] Kei Yamamoto,[2,*] Maki Umeda,[2,3] Christoph W. Zollitsch,[1] Mehrdad Elyasi,[4] Takashi Kikkawa,[5] Eiji Saitoh,[2,4,5,6] Gerrit E. W. Bauer,[4,7] and Hidekazu Kurebayashi[1,4,8,†]

[1]*London Centre for Nanotechnology, University College London, London WC1H 0AH, United Kingdom*
[2]*Advanced Science Research Center, Japan Atomic Energy Agency, 2-4 Shirakata, Tokai 319-1195, Japan*
[3]*Institute for Materials Research, Tohoku University, Sendai 980-8577, Japan*
[4]*WPI Advanced Institute for Materials Research, Tohoku University, 2-1-1, Katahira, Sendai 980-8577, Japan*
[5]*Department of Applied Physics, The University of Tokyo, Tokyo 113-8656, Japan*
[6]*Institute for AI and Beyond, The University of Tokyo, Tokyo 113-8656, Japan*
[7]*Kavli Institute for Theoretical Sciences, University of the Chinese Academy of Sciences, Beijing 100190, China*
[8]*Department of Electronic and Electrical Engineering, University College London, London WC1E 7JE, United Kingdom*

(Received 25 January 2022; revised 19 September 2022; accepted 7 December 2022; published 26 January 2023)

We experimentally and theoretically demonstrate that nonlinear spin-wave interactions suppress the hybrid magnon-photon quasiparticle or "magnon polariton" in microwave spectra of a yttrium iron garnet film detected by an on-chip split-ring resonator. We observe a strong coupling between the Kittel and microwave cavity modes in terms of an avoided crossing as a function of magnetic fields at low microwave input powers, but a complete closing of the gap at high powers. The experimental results are well explained by a theoretical model including the three-magnon decay of the Kittel magnon into spin waves. The gap closure originates from the saturation of the ferromagnetic resonance above the Suhl instability threshold by a coherent backreaction from the spin waves.

DOI: 10.1103/PhysRevLett.130.046703

The spectral properties of many-body systems can often be understood in terms of weakly interacting quasiparticles. When tuning the energies of two elementary excitations into degeneracy by an external parameter, their coupling leads to a level repulsion. When the resultant gap is larger than the level broadening, it becomes observable in the spectrum. This so-called strong coupling generates a hybrid quasiparticle that shares the properties of both ingredients. The strong coupling between magnons, phonons, photons, excitons, plasmons, etc., has important consequences and applications in condensed matter physics [1–6]. Here we address the magnon polariton, i.e., the mixed state of a spin wave in a ferromagnet and a microwave magnetic field [7–10]. While magnon polaritons are often discussed in the context of quantum computing by discrete qubits [11], they are more generally relevant for the control of continuous magnon variables by electromagnetic fields. Although they have been extensively studied in the linear response regime of weak microwave excitation, their nonlinearities have so far escaped similar attention.

In comparison, nonlinearities in magnetic excitations have been known for many decades [12–14]. They can be useful in, for instance, probabilistic bits [15,16], and offer continuous variables with controllable squeezing and entanglement that act as resources in quantum information [17,18]. The magnon nonlinearities can be treated systematically by the Holstein-Primakoff power expansion of a spin Hamiltonian in creation and annihilation operators $b_{\boldsymbol{k}}^{\dagger}, b_{\boldsymbol{k}}$. With increasing excitation, progressively higher-order terms of the expansion become important. We focus on the three-magnon scattering; the leading nonlinear term that involves the splitting of a magnon into two and the reciprocal confluence [13,19]. The interaction causes the first-order Suhl instability of a uniform precession of the magnetic order, or Kittel mode represented by b_0, at a threshold power that can be very small in low-damping magnets [19–26]. Figure 1(a) illustrates the scattering process in which a Kittel magnon excited by ferromagnetic resonance (FMR) decays

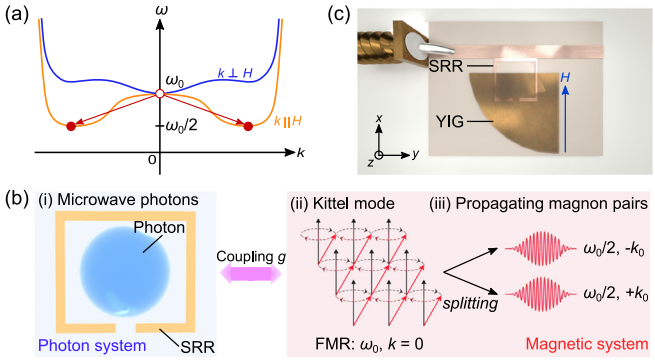

FIG. 1. (a) Spin-wave dispersion of a YIG film. Red arrows indicate the split of a Kittel magnon with the frequency ω_0 into two magnons of frequency $\omega_0/2$. (b) Schematic of the magnon polariton with the spin-wave instability as explained in the main text. (c) Measurement setup.

into two magnons of half its frequency and opposite momenta $\pm\boldsymbol{k}$. This three-magnon splitting is allowed only when magnetic dipole-dipole interactions render a nonmonotonic magnonic dispersion with minima at half the Kittel mode frequency or below. When the Kittel mode is excited, the three-magnon splitting pumps the magnon pair amplitude $\langle b_{\boldsymbol{k}} b_{-\boldsymbol{k}}\rangle$ at a rate proportional to that of the Kittel mode $|\langle b_0\rangle|$. When the pumping rate exceeds the relaxation rate of the magnons $\eta_{\boldsymbol{k}}$, a nonthermal magnon population accumulates in the valleys of the magnon dispersion. This first-order Suhl instability manifests itself in microwave reflection spectra by, e.g., distortions of the spectral line shape from a Lorentzian [13].

In this Letter, we study this nonlinear instability under the condition that the Kittel magnon strongly couples to the photon in a discrete microwave cavity [Fig. 1(b)]. Since magnon-photon coupling can be used to read information out or distill entanglement in these applications, nonlinear magnon-polariton phenomena may become a crucial ingredient in novel computing and information-technology paradigms [7,16,17]. Our main result is the observation and modeling of the suppression of the strong-coupling gap by the instability. The nonlinear spin-wave equation coupled to the cavity mode explains our observations in terms of the saturation of the Kittel mode by a dynamical phase correlation between the cavity photons and the magnon pairs in the valleys. To the best of our knowledge, a tunable strong coupling has not been reported for magnon polaritons and adds to the appeal of magnetic materials for classical and quantum information technologies [7,17,27].

We study a 5-μm-thick yttrium iron garnet (YIG) film grown on a gadolinium gallium garnet substrate by liquid-phase epitaxy [28–30] and placed on a split-ring microwave resonator (SRR) as depicted in Fig. 1(c) [31,32]. We measured microwave absorption or reflection spectra $|S_{11}|$ at room temperature using a vector network analyzer. Figure 2(a) shows $|S_{11}|$ for different input microwave powers P as a function of frequency $\omega/2\pi$ and magnetic

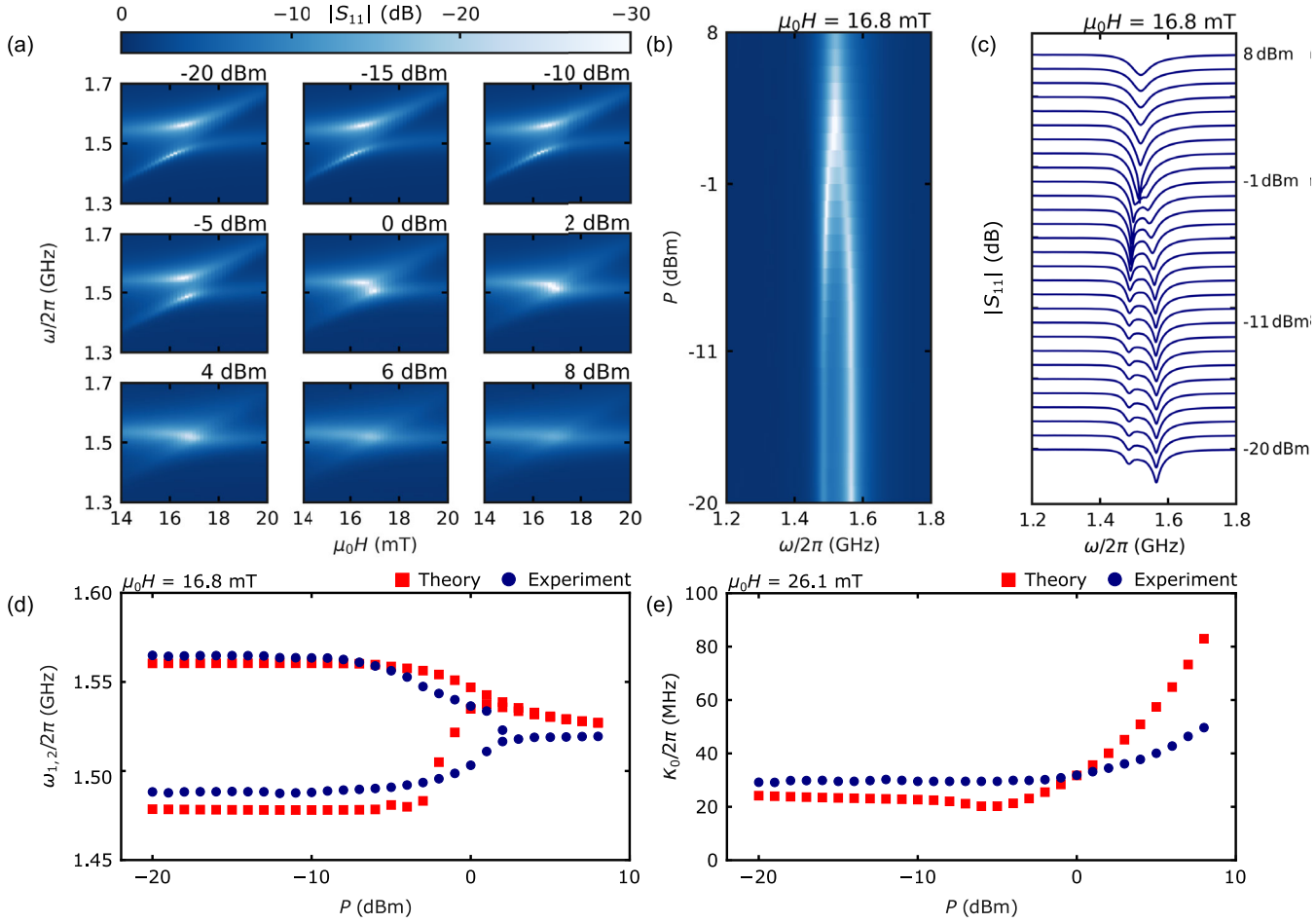

FIG. 2. (a) Microwave absorption spectra [$|S_{11}|$ (dB)] as a function of microwave frequency and magnetic field strength, for different microwave power ranging from −20 to 8 dBm. (b),(c) Collection of frequency domain scans for a fixed magnetic field of 16.8 mT. (d) Comparison between measured and calculated gaps. Peak frequencies are extracted from individual fits for different microwave powers. (e) Microwave power evolution of the observed and calculated linewidths of the Kittel mode in the weak-coupling regime ($\mu_0 H = 26.1$ mT).

field $\mu_0 H$. For $P = -20$ dBm, a prominent avoided crossing between the Kittel mode frequency $\omega_0/2\pi$ and the cavity photon mode $\omega_r/2\pi \approx 1.5$ GHz is evidence for strong magnon-photon coupling. The minimum frequency difference, half of which is the coupling strength $g/2\pi = 41$ MHz, occurs at the resonance field $\mu_0 H_{\rm res} = 16.8$ mT. In linear response, $|g| = \eta\gamma\sqrt{\hbar\mu_0\omega_r}\sqrt{N/\mathcal{V}_c}$, where η, γ, $\hbar$, μ_0, N, and $\mathcal{V}_c$ are the filling factor that characterizes the spatial mode overlap between the photon and magnon modes, the gyromagnetic ratio, reduced Planck constant, vacuum permeability, number of spins, and the cavity mode volume, respectively [7]. The individual linewidths of the photon and magnon are obtained by Lorentzian function fittings of the respective resonances $\kappa_r(\kappa_0)/2\pi = 52.0(28.0)$ MHz at $\mu_0 H = 26.1$ mT far from the avoided crossing. With increasing P, the avoided-crossing gap narrows and the two peaks eventually merge [Fig. 2(a)]. Figures 2(b) and 2(c) show that the two peaks on resonance $H = H_{\rm res}$ coalesce into a single one at high powers, seemingly canceling the magnon-photon coupling. Figure 2(d) summarizes the frequencies of the peaks in the spectra, illustrating the vanishing of the gap that constitutes our main result. As argued in the following, we attribute it to the first-order Suhl instability.

The Suhl instability alters magnetic susceptibility [19,33,34] and line shape [13] by the nonlinear back-reaction of the excited magnon pairs on the Kittel magnon. We confirm an implied increased broadening by measuring the P dependence of the Kittel mode linewidth at $\mu_0 H = 26.1$ mT $> \mu_0 H_{\rm res}$, far away from the cavity resonance. As shown in Fig. 2(e), we observe an increase in broadening for $P \gtrsim 0$ dBm, which is expected for entering the power regime of the first-order Suhl instability. The critical number of Kittel magnons per spin at the threshold is $|\langle b_0\rangle|^2/N = \text{const} \times \eta_{\boldsymbol{k}}^2/\omega_M^2$, where $\omega_M = \gamma\mu_0 M_s$ is the saturation magnetization. The difference between the onset powers for the gap closure in Fig. 2(d) and the broadening in Fig. 2(e) implies that the dimensionless constant of order unity depends on the system parameters including H and ω.

We can corroborate our interpretation by increasing H to couple the Kittel mode with a higher SRR cavity mode. Energy conservation $\omega_0 = 2\omega_{\boldsymbol{k}}$, where $\omega_{\boldsymbol{k}}$ is the frequency of a magnon with wave vector $\boldsymbol{k}$, demands that $\omega_0 \geq 2\omega_b$ where ω_b is the band edge frequency. Since both ω_0 and ω_b increase roughly linearly with H, the three-magnon splitting is forbidden above a critical field value $H_{\rm cr}$, at which $\omega_0(H_{\rm cr})/2\pi = 2.59$ GHz for our YIG sample with a thickness of 5 μm, $M_s = 1.26 \times 10^5$ A/m, and a stiffness constant of $\lambda_{\rm ex} = 3 \times 10^{-16}$ m^2 [35] [see Supplemental Material (SM) [36]]. The magnon polariton of the 3.0 (3.5) GHz SRR mode in Fig. 3(a) (in Fig. S5 in SM [36]) should therefore depend much less on the microwave power. By increasing P up to 8 dBm as before, the reflection spectrum [Fig. 3(b)] and the fixed-field plot in Fig. 3(c) confirm that the avoided-crossing gap does not vanish and the Kittel mode linewidth in Fig. 3(d) remains unchanged, which supports our hypothesis that the Suhl instability explains Fig. 2.

We substantiate the above arguments by the kinetic theory of nonlinear spin-wave dynamics [13,39] extended to incorporate the magnon polariton. We start from the model Hamiltonian $\mathcal{H} = \mathcal{H}_1 + \mathcal{H}_2 + \mathcal{H}_3$ (in frequency units), in which

$$\mathcal{H}_2 = \omega_r b_r^\dagger b_r + [g b_0^\dagger b_r + \text{H.c.}] + \omega_0 b_0^\dagger b_0 + \sum_{\boldsymbol{k}\neq\boldsymbol{0}} \omega_{\boldsymbol{k}} b_{\boldsymbol{k}}^\dagger b_{\boldsymbol{k}} \quad (1)$$

describes noninteracting fields as coupled harmonic oscillators, where b_r is the annihilation operator for the selected cavity photon, and ω_r is its frequency. The microwave stripline drive contributes

$$\mathcal{H}_1 = [h e^{-i\omega t}(U_r b_r^\dagger + U_0 b_0^\dagger) + \text{H.c.}], \quad (2)$$

where h and ω are the amplitude (in frequency units) and frequency of the stripline field, and U_0 and U_r are its (dimensionless) coupling strengths to the Kittel and cavity mode, respectively. The nonlinear coupling $V_{\boldsymbol{k}} \sim \omega_M/\sqrt{N}$ in

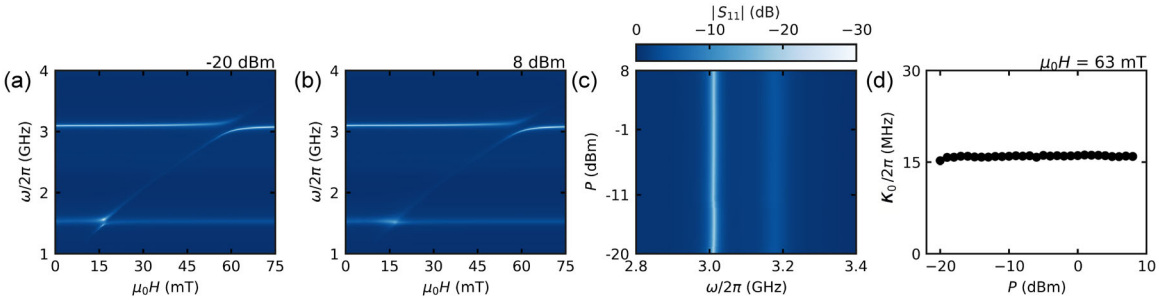

FIG. 3. $|S_{11}|$ as a function of microwave frequency and magnetic field strength, for low (a) and high (b) microwave powers. (c) Microwave absorption spectra for the 3.0 GHz SRR mode at a fixed magnetic field of 60 mT, at which the frequency difference between the two peaks is the smallest. (d) Power evolution of Kittel mode linewidth (κ_0) at a fixed magnetic field above the avoided crossing (63 mT) for the 3.0 GHz SRR mode.

$$\mathcal{H}_3 = \frac{1}{2}\sum_{k\neq 0} \overline{V_k}\, b_0 b_k^\dagger b_{-k}^\dagger + \text{H.c.} \tag{3}$$

is a function of the material parameters [13]. Overlines denote complex conjugation throughout. We omitted four-magnon scattering terms because in the present setup the critical power of the first-order Suhl instability is much smaller than the second-order one (see SM [36]). At room temperature, one may safely interpret the field operators as classical amplitudes with thermal fluctuations. In the film geometry with an in-plane static magnetic field, only a narrow band of magnons are involved in the onset of the instabilities [40], which we approximate here by the single pair $\pm\boldsymbol{k}\|\boldsymbol{H}$ with smallest $\eta_k/|V_k|$. The steady-state solutions are characterized by the thermal averages $\langle b_{0,r}\rangle$ and $\langle b_k b_{-k}\rangle$. The coherent amplitude of the Kittel mode $\langle b_0\rangle$ is a root of a (complex) cubic algebraic equation [Eq. (S25) in the SM [36]], which at sufficiently high powers $|h| \to \infty$ approaches

$$\langle b_0\rangle \to -e^{-i\omega t + i\psi_k}\overline{c_{\rm cr}}, \quad c_{\rm cr} = \frac{\omega_k - \omega/2 + i\eta_k}{V_k}, \tag{4}$$

where ψ_k is the phase of the magnon pair amplitude $\langle b_k b_{-k}\rangle$. The absence of h on the rhs implies *saturation*, i.e., the number of Kittel magnons n_0 cannot exceed the critical value $|c_{\rm cr}|^2$, which depends only on the magnonic parameters. Furthermore (for all $|h|$),

$$\langle b_r\rangle = \frac{\bar{g}\langle b_0\rangle + hU_r e^{-i\omega t}}{\omega - \omega_r + i\kappa_r}, \tag{5}$$

$$\langle b_k b_{-k}\rangle = -\frac{c_{\rm cr}\langle b_0\rangle}{|c_{\rm cr}|^2 - |\langle b_0\rangle|^2}\frac{k_B T}{\hbar\omega_k}, \tag{6}$$

where T is the temperature and k_B the Boltzmann constant. Photon and magnon pair amplitudes coherently oscillate with the Kittel mode, whose phase in turn locks to that of the driving field h. The saturation limit Eq. (4) is valid in a nonvanishing interval above the critical power [40] and explains the main features of the observations.

Figures 4(a) and 4(b) summarize the theoretical results with the standard parameters for YIG, i.e., an extracted saturation magnetization $M_s = 1.26\times10^5$ A/m for $\gamma/2\pi =$ 28 GHz/T, and a magnetic-relaxation-rate parameter $\kappa_0/2\pi = 22$ MHz. We model the microwaves system by $\omega_r/2\pi = 1.53$ GHz, $\kappa_r/2\pi = 52$ MHz, $U_r = 0.95\times e^{0.4i\pi}$, and $U_0 = 0.31$. We take magnon-photon coupling $g/2\pi =$ 41 MHz directly from the gap of the avoided crossing at low P. The Kittel formula is $\omega_0 = \mu_0\gamma\sqrt{H(H+M_s)}$. For the coherently coupled magnon pair at $\omega_k = \omega/2$, we assume $\eta_k = 0.01\times\omega_0/2$ and $V_k = \omega_M\times10^{-11/2}$ (see SM [36]). The calculated spectra compare favorably with the observed gap closure and the line shapes [Figs. 2(d) and 2(e)]. Considering the simplifications made in the model [36] that always tend to predict a faster development of instability with more extreme spectral distortions, the agreement is satisfactory. It reproduces the asymmetry between the avoided-crossing peaks at low powers, which is caused by the broadening [36]. Note that the spectra at high powers cannot be explained by the dissipative coupling observed in very different regimes in Refs. [41,42]. We can instead attribute the quenching of the avoided crossing to the saturation of the Kittel mode [Eq. (4)]. Below the critical power, a photon injected into the cavity

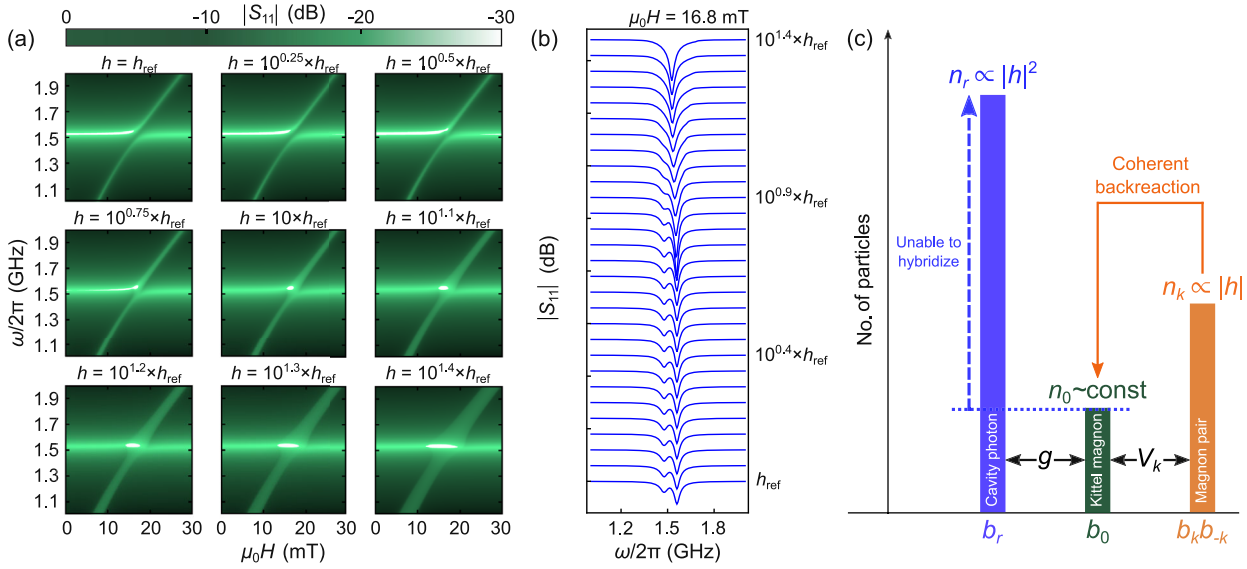

FIG. 4. (a) Microwave reflection spectrum $|S_{11}|$ (defined in the Supplemental Material [36]) calculated from Eqs. (4) and (5) for model parameters in the text and an arbitrary reference input power $h_{\rm ref}$. (b) $|S_{11}|$ at $\mu_0 H = 16.8$ mT. (c) Schematic of the particle number growth with h for magnon polaritons beyond the Suhl instability.

mixing with a Kittel magnon causes the avoided crossing. Above the critical power, however, cavity photons are much more numerous than the Kittel magnons limited by the coherent backreaction from the magnon pairs, as illustrated in Fig. 4(c). The excess photons become effectively decoupled and therefore do not show the avoided crossing. Their spectral characteristics overwhelm the gap opened by the few saturated magnons, thereby causing an apparent closure of the gap.

In summary, we discovered suppression of the strong magnon-photon coupling in highly excited microwave cavities at the first-order Suhl instability. The closure of the hybridization gap calculated with a nonlinear spin-wave model coupled to a microwave cavity photon mode agrees quantitatively with the observations. This effect is a result of the phase coherence between the photons and the entire spin-wave system that saturates the number of Kittel magnons under large microwave drives. The ability to coherently excite or detect magnon pairs in the low energy valleys not only contributes to studying and controlling quantum entanglement of magnons [17,18], but also opens new avenues in magnonics, such as the microwave spectroscopy of magnon Bose-Einstein condensates [43]. The present Letter promises ample room for unexpected discoveries in nonlinear magnonics as an exciting research frontier.

K. Y. is supported by JST PRESTO Grant No. JPMJPR20LB, Japan and JSPS KAKENHI (No. 19K21040 and No. 21K13886), G. E. W. B. by JSPS KAKENHI Grant No. 19H00645, and T. K. and E. S. by JST CREST (JPMJCR20C1 and JPMJCR20T2), JSPS KAKENHI (JP19H05600 and JP20H02599), as well as the Institute for AI and Beyond of the University of Tokyo. M .U. was supported by JSPS through a research fellowship for young scientists (No. JP19J13544) and GP-Spin at Tohoku University. M. U. is also supported by JSPS KAKENHI (No. JP22K14593). We thank C. Dubs of INNOVENT e.V. Jena, Germany, for providing additional YIG films.

*yamamoto.kei@jaea.go.jp
†h.kurebayashi@ucl.ac.uk

[1] S. Haroche and J.-M. Raimond, *Exploring the Quantum: Atoms, Cavities, and Photons* (Oxford University Press, Oxford, 2006), 10.1093/acprof:oso/9780198509141.001.0001.
[2] R. J. Schoelkopf and S. M. Girvin, Nature (London) **451**, 664 (2008).
[3] D. S. Dovzhenko, S. V. Ryabchuk, Y. P. Rakovich, and I. R. Nabiev, Nanoscale **10**, 3589 (2018).
[4] P. Forn-Díaz, L. Lamata, E. Rico, J. Kono, and E. Solano, Rev. Mod. Phys. **91**, 025005 (2019).
[5] D. N. Basov, M. M. Fogler, and F. J. G. de Abajo, Science **354**, aag1992 (2016).
[6] D. A. Bozhko, V. I. Vasyuchka, A. V. Chumak, and A. A. Serga, Low Temp. Phys. **46**, 383 (2020).
[7] B. Z. Rameshti, S. V. Kusminskiy, J. A. Haigh, K. Usami, D. Lachance-Quirion, Y. Nakamura, C.-M. Hu, H. X. Tang, G. E. W. Bauer, and Y. M. Blanter, Phys. Rep. **979**, 1 (2022).
[8] M. Harder, B. M. Yao, Y. S. Gui, and C.-M. Hu, J. Appl. Phys. **129**, 201101 (2021).
[9] D. Lachance-Quirion, Y. Tabuchi, A. Gloppe, K. Usami, and Y. Nakamura, Appl. Phys. Express **12**, 070101 (2019).
[10] D. D. Awschalom *et al.*, IEEE Trans. Quantum Eng. **2**, 1 (2021).
[11] Y. Tabuchi, S. Ishino, T. Ishikawa, R. Yamazaki, K. Usami, and Y. Nakamura, Phys. Rev. Lett. **113**, 083603 (2014).
[12] N. Bloembergen and R. W. Damon, Phys. Rev. **85**, 699 (1952).
[13] V. S. L'vov, *Wave Turbulence Under Parametric Excitation* (Springer-Verlag, Berlin, 1994), 10.1007/978-3-642-75295-7.
[14] P. E. Wigen, *Nonlinear Phenomena and Chaos in Magnetic Materials* (World Scientific, Singapore, 1994), 10.1142/1686.
[15] T. Makiuchi, T. Hioki, Y. Shimazu, Y. Oikawa, N. Yokoi, S. Daimon, and E. Saitoh, Appl. Phys. Lett. **118**, 022402 (2021).
[16] M. Elyasi, E. Saitoh, and G. E. W. Bauer, Phys. Rev. B **105**, 054403 (2022).
[17] H. Yuan, Y. Cao, A. Kamra, R. A. Duine, and P. Yan, Phys. Rep. **965**, 1 (2022).
[18] M. Elyasi, Y. M. Blanter, and G. E. W. Bauer, Phys. Rev. B **101**, 054402 (2020).
[19] H. Suhl, Phys. Chem. Solids **1**, 209 (1957).
[20] V. T. Synogach, Y. K. Fetisov, C. Mathieu, and C. E. Patton, Phys. Rev. Lett. **85**, 2184 (2000).
[21] C. Mathieu, V. T. Synogatch, and C. E. Patton, Phys. Rev. B **67**, 104402 (2003).
[22] C. L. Ordóñez-Romero, B. A. Kalinikos, P. Krivosik, W. Tong, P. Kabos, and C. E. Patton, Phys. Rev. B **79**, 144428 (2009).
[23] H. Schultheiss, X. Janssens, M. van Kampen, F. Ciubotaru, S. J. Hermsdoerfer, B. Obry, A. Laraoui, A. A. Serga, L. Lagae, A. N. Slavin, B. Leven, and B. Hillebrands, Phys. Rev. Lett. **103**, 157202 (2009).
[24] H. Kurebayashi, O. Dzyapko, V. E. Demidov, D. Fang, A. J. Ferguson, and S. O. Demokritov, Nat. Mater. **10**, 660 (2011).
[25] H. Sakimura, T. Tashiro, and K. Ando, Nat. Commun. **5**, 5730 (2014).
[26] I. Barsukov, H. K. Lee, A. A. Jara, Y.-J. Chen, A. M. Gonçalves, C. Sha, J. A. Katine, R. E. Arias, B. A. Ivanov, and I. N. Krivorotov, Sci. Adv. **5**, eaav6943 (2019).
[27] A. Mahmoud, F. Ciubotaru, F. Vanderveken, A. V. Chumak, S. Hamdioui, C. Adelmann, and S. Cotofana, J. Appl. Phys. **128**, 161101 (2020).
[28] C. Dubs, O. Surzhenko, R. Linke, A. Danilewsky, U. Brückner, and J. Dellith, J. Phys. D **50**, 204005 (2017).
[29] C. Dubs, O. Surzhenko, R. Thomas, J. Osten, T. Schneider, K. Lenz, J. Grenzer, R. Hübner, and E. Wendler, Phys. Rev. Mater. **4**, 024416 (2020).
[30] T. Kikkawa, K. Oyanagi, T. Hioki, M. Ishida, Z. Qiu, R. Ramos, Y. Hashimoto, and E. Saitoh, Phys. Rev. Mater. **6**, 104402 (2022).

[31] G. B. G. Stenning, G. J. Bowden, L. C. Maple, S. A. Gregory, A. Sposito, R. W. Eason, N. I. Zheludev, and P. A. J. de Groot, Opt. Express **21**, 1456 (2013).
[32] B. Bhoi, T. Cliff, I. S. Maksymov, M. Kostylev, R. Aiyar, N. Venkataramani, S. Prasad, and R. L. Stamps, J. Appl. Phys. **116**, 243906 (2014).
[33] R. W. Damon, Rev. Mod. Phys. **25**, 239 (1953).
[34] N. Bloembergen and S. Wang, Phys. Rev. **93**, 72 (1954).
[35] A. Prabhakar and D. D. Stancil, *Spin Waves: Theory and Applications* (Springer, New York, 2009), 10.1007/978-0-387-77865-5.
[36] See Supplemental Material at http://link.aps.org/supplemental/10.1103/PhysRevLett.130.046703, which includes Refs. [37,38], for the basic characteristics of spin waves in a YIG film (Sec. II); the theoretical details of the Suhl instability, the rational behind the choice of the parameters, and the simplifying assumptions in the theoretical model (Sec. IV); and the effect of broadening on avoided-crossing line shapes (Sec. V).
[37] B. A. Kalinikos, Sov. Phys. J. **24**, 718 (1981).
[38] V. E. Zakharov, G. Falkovich, and V. S. L'vov, *Kolmogorov Spectra of Turbulence I: Wave Turbulence* (Springer, Berlin, 1992), 10.1007/978-3-642-50052-7.
[39] H. Suhl and X. Y. Zhang, J. Appl. Phys. **63**, 4147 (1988).
[40] V. E. Zakharov, V. S. L'vov, and S. S. Starobinets, Sov. Phys. Usp. **17**, 896 (1975).
[41] M. Harder, Y. Yang, B. M. Yao, C. H. Yu, J. W. Rao, Y. S. Gui, R. L. Stamps, and C.-M. Hu, Phys. Rev. Lett. **121**, 137203 (2018).
[42] I. Boventer, C. Dörflinger, T. Wolz, R. Macêdo, R. Lebrun, M. Kläui, and M. Weides, Phys. Rev. Res. **2**, 013154 (2020).
[43] S. O. Demokritov, V. E. Demidov, O. Dzyapko, G. A. Melkov, A. A. Serga, B. Hillebrands, and A. N. Slavin, Nature (London) **443**, 430 (2006).